LA-UR -86-421
CONF-851027--1

Los Alamos National Laboratory is operated by the University of California for the United States Department of Energy under contract W-7405-ENG-36.

LA-UR--86-421

DE86 006046

TITLE: THE MICROSTRUCTURAL DYNAMICS OF PRIMARY AND SECONDARY RECRYSTALLIZATION

AUTHOR(S): M. P. Anderson
G. S. Grest
D. J. Srolovitz

SUBMITTED TO: The proceedings of the "Computer Simulation of Microstructural Evolution, Symposium," held in Toronto, Canada, October 14-17, 1985.

DISCLAIMER

MASTER

Los Alamos Los Alamos National Laboratory
Los Alamos, New Mexico 87545

FORM NO 836 R4
ST NO 2629 5/81

THE MICROSTRUCTURAL DYNAMICS OF PRIMARY AND SECONDARY RECRYSTALLIZATION

M. P. Anderson*, G. S. Grest* and D. J. Srolovitz#

*Corporate Research Science Laboratory
Exxon Research and Engineering Company
Annandale, NJ 08801

#Theoretical Division
Los Alamos National Laboratory
Los Alamos, New Mexico 87545

Monte Carlo computer simulation techniques have been applied to the problem of recrystallization in a two dimensional matrix. Both primary and secondary recrystallization are investigated. Primary recrystallization is modelled under conditions where the degree of stored energy is varied and nucleation occurs either continuously as a function of time or as site saturated. The degree of stored energy is adjusted to range from heterogeneous nucleation at grain edges and corners to homogeneous nucleation throughout the microstructure. Secondary recrystallization is modelled: (a) where the driving force is provided solely by curvature and (b) where the driving force is provided by the difference in the solid-vapor surface energy between grains of different crystallographic orientation. The role of particles in initiating secondary recrystallization is also addressed. The microstructure and kinetics for the different recrystallization processes are discussed and compared.

Introduction

The complete prediction of microstructural development in polycrystalline solids as a function of time and temperature is a major objective in materials science, but has not yet been possible primarily due to the complexity of the grain interactions. The evolution of the polycrystalline structure depends upon the precise specification of the coordinates of the grain boundary network, the crystallographic orientations of the grains, and the postulated microscopic mechanisms by which elements of the boundaries are assumed to move. Therefore, a general analytical solution to this multivariate problem has not yet been developed. Recently, we have been able to successfully incorporate these aspects of the grain interactions, and have developed a computer model which predicts the main features of the microstructure from first principles (1,2). The polycrystal is mapped onto a discrete lattice by dividing the material into small area (2d) or volume (3d) elements, and placing the centers of these elements on lattice points. This discrete model preserves the topological features of real systems, and can be studied by computer simulation using Monte Carlo techniques. The application of the model to normal grain growth with isothermal annealing is presented elsewhere in this volume (3). In this paper we will review extension of the model to treat primary and secondary recrystallization.

Primary recrystallization is the process in which a deformed metal is transformed into a strain-free structure by the nucleation and growth of strain-free grains (4). The dominant driving force for this phenomenon is assumed to be excess energy distributed in the interior of the deformed grains, in the form of point defects and dislocations. Experimentally it is often observed that the recrystallized volume fraction F exhibits a sigmoidal dependence on time (5). This type of dependence can often be fit by a simple mathematical relationship derived by Johnson and Mehl (6), and Avrami (7) (JMA):

$$F = 1 - \exp(-At^p) \qquad (1)$$

where A and p are constants. An important difference which exists between recrystallization and normal grain growth is that the motion of the recrystallized boundaries is dominated by the volume (3d) or area (2d) distributed energies. As a first attempt to directly correlate microstructural development with this type of driving force, the temporal evolution of microstructure is examined as a function of the nucleation rate and stored energy density. Primary recrystallization is modelled under conditions where the degree of stored energy is varied and nucleation occurs either heterogeneously or homogeneously. The nucleation rate is chosen as either constant or site saturated. Details of the nucleation mechanism are not, however, investigated in the present study.

Grain growth is the term used to describe the increase in grain size which occurs upon annealing after primary recrystallization is complete. At least two different types of grain growth phenomena have been distinguished. Normal grain growth is said to occur when the microstructure exhibits a uniform increase in size (8). This process has been treated in a companion paper (3). The second type of growth which can take place is secondary recrystallization. In the present context, secondary recrystallization refers to the rapid increase in size of a few grains in the recrystallized microstructure such that the maximum grain size increases at a rate much faster than the arithmetic mean (9). This type of growth is similar to primary recrystallization in that the volume fraction of secondary grains often exhibits sigmoidal time dependence, and can be fit by the JMA relationship (Eq.1). At least two different origins

for secondary recrystallization have been suggested. In the first it is assumed that the driving force for growth is derived solely from the decrease in total grain boundary energy (curvature) (10-12). Secondary recrystallization then occurs as a consequence of growth instabilities predicted under a restricted set of conditions by mean field treatments of grain growth. The second explanation postulates that, in addition to curvature, a volume (3d) or area (2d) distributed excess energy must be present (13-15). Secondary recrystallization then initiates as a consequence of local differences in the volume distributed energy. For 2d materials (sheets and thin films), experimental evidence indicates that one source of this additional driving force is the orientation dependence of the solid-vapor surface energies for the recrystallized grains. In an attempt to check the validity of these alternatives, the growth of abnormally large grains in a two-dimensional matrix is modelled under two conditions: (a) where the driving force is provided solely by curvature and (b) where the driving force is provided by the difference in the solid-vapor surface energy between grains of different crystallographic orientation.

Procedure

The procedures employed in the simulations are described in Ref. 16 for primary recrystallization, and Ref. 17 for secondary recrystallization. In short, a continuum microstructure is mapped onto a two dimensional triangular lattice containing 40,000 lattice sites. Each lattice site is assigned a number, S_i, which corresponds to the orientation of the grain in which it is embedded. The number of distinct grain orientations is Q. Lattice sites which are adjacent to neighboring sites having different grain orientations are regarded as being part of the grain boundary, whilst a site surrounded by sites with the same grain orientation is in the grain interior.

The site energy, E_i, is defined to be the sum of two contributions, E_i^I and E_i^{II}. The grain boundary energy is specified by E_i^I

$$E_i^I = -J \sum_{nn} (\delta_{S_i S_j} - 1) \qquad (2)$$

where $\delta_{i,j}$ is the Kronecker delta, the sum is taken over the nearest neighbor (nn) sites and J is a positive constant that sets the scale of the grain boundary energy. E_i^{II} specifies the energy stored within the grain interior due to deformation or (in 2d) to the solid-vapor surface energy.

To treat primary recrystallization, E_i^{II} is defined to be a positive energy such that

$$E_i^{II} = H\, \theta(Q_u - S_i) \qquad (3)$$

where $\theta(x) = 1$ for $x \geq 0$ and $= 0$ for $x < 0$. H is a positive constant which sets the magnitude of the stored energy and Q_u is the number of distinct orientations of unrecrystallized grains. Strain-free grains are nucleated in the microstructure under conditions described in the results section below. These recrystallized nuclei are given orientations with $S_i > Q_u$, such that the S_i for a given recrystallized nucleus is shared by no other grains or nuclei.

To treat secondary recrystallization, E_i^{II} is defined to be a negative energy such that

$$E_i^{II} = -H \sum_k \delta_{S_i\, Q_k} \qquad (4)$$

H is a positive constant which sets the magnitude of the solid-vapor surface energy. In simulations of secondary recrystallization where curvature is used as the only driving force, H=0. For those simulations where surface energy is employed as an additional driving force, H>0. If, in a given annealing atmosphere, certain grains have a lower total energy than surrounding grains due to the dependence of surface energy on the crystallographic orientation of the surface plane, it is speculated that these grains will grow faster - resulting in secondary recrystallization (13-15). H scales the amount by which the surface energy of a grain having orientation S_i is lowered. The summation in Eq. 4 is over the set of orientations Q_k, which is a list of favored grain orientations chosen at random at the start of the simulation from the Q total orientations of the recrystallized microstructure. The delta function in Eq. 4 is one if S_i in one of the favored orientations, and zero if it is not.

The kinetics of the boundary motion are simulated employing a Monte Carlo procedure in which a lattice site is selected at random and its orientation is randomly changed to one of the other grain orientations. The change in energy, ΔE, associated with the change in orientation is evaluated. If the change in energy is less than or equal to zero, the re-orientation is accepted. However, if the change in energy is greater than zero, the re-orientation is accepted with the probability $\exp(-\Delta E/kT)$. Time, in these simulations, is related to the number of re-orientation attempts. N re-orientation attempts is arbitrarily used as the unit of time and is referred to as 1 Monte Carlo Step (MCS), where N is the number of lattice sites (40,000). The conversion from MCS to real time has an implicit activation energy factor, $\exp(-W/kT)$, which corresponds to the atomic jump frequency. Since the quoted times are normalized by the jump frequency, the only effect of choosing T=0 (as done in the present simulations) is to restrict the accepted re-orientation attempts to those which lower the energy of the system. Re-orientation of a site at a grain boundary corresponds to boundary migration. The boundary velocity determined in this manner yields kinetics that are formally equivalent to the rate theory model.

Results and Discussion

A. Primary Recrystallization

In classical homogeneous nucleation theory the minimum radius of a spherical nucleus which will grow is $2\gamma/\delta G$, where γ is the surface energy per unit area and δG is the difference between the energy stored in the nucleus and that stored in the surrounding matrix (normalized per unit volume). In the present simulations, the minimum nucleus radius which will grow but cannot shrink without regard to location in the microstructure is proportional to J/H, where the proportionality constant depends upon the nucleus shape. While the critical nucleus size in a continuum system is a continuous function of J/H, on a discrete lattice at T=0 the critical size changes discontinuously. On a triangular lattice the critical nucleus size is one site for $H/J>4$, three sites for $4>H/J>2$, and essentially infinite for $2>H/J>0$. For $H/J<2$, the nucleation can only be heterogeneous.

For metallic systems undergoing recrystallization, the ratio H/J is in the range 0.01 to 0.1 (18). In the present simulations H/J was selected to range from 0.1 to 5.0. Although these values are in excess of those observed in metals, they are required in the discrete lattice model to vary between heterogeneous to homogeneous nucleation and growth behavior.

1. Circular Grains

The behavior of individual, growing, recrystallized grains in a uniform background was investigated first. The temporal evolution of the recrystallized grains for two values of stored energy, H/J=3 and H/J=5, are shown in Fig. 1. Three significant features are found. First, the grains

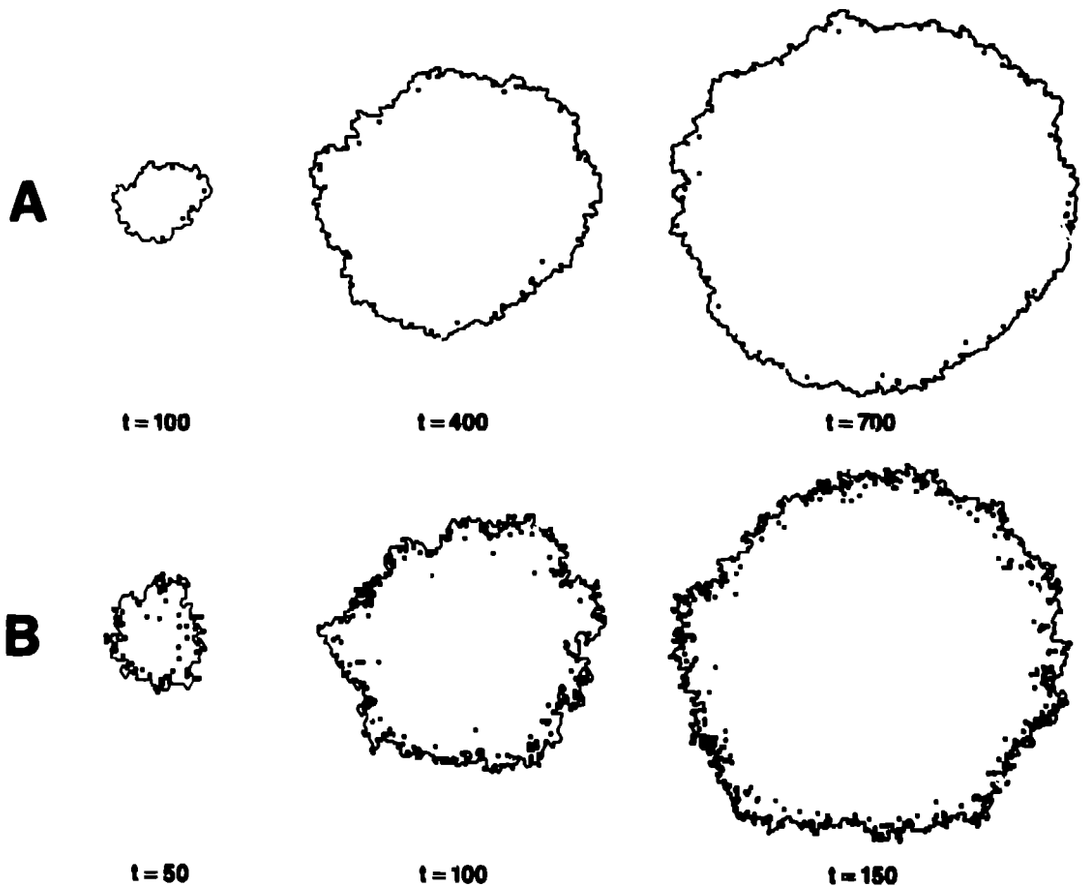

Fig. 1 The growth of a circular grain in a uniform background (a) H/J=3 and (b) H/J=5.

evolve such that the grain shape remains nearly circular. This indicates that the grain boundary mobility is isotropic and insensitive to the symmetry of the underlying lattice. Second, the rate of growth increases asymptotically with time squared. This is consistent with exact analytical solutions for this simple geometry, and verifies that the boundary migration kinetics are properly incorporated. Finally, the grain boundaries are not perfectly smooth, but exhibit a small degree of roughness. The magnitude of the roughness increases with stored energy. This is regarded as a finite size effect in the model, which is due to the discreteness and low dimensionality of the simulation. The scale of roughness does not increase with the size of the grain, and hence the normalized roughness decays with increasing domain size.

2. Homogeneous Nucleation

The recrystallization of a polycrystalline matrix under conditions of homogeneous nucleation was investigated next. By homogeneous nucleation is meant that the degree of stored energy is high enough that an embryo of critical size will grow in a uniform background. For these simulations,

the microstructure was initialized by a 1000 MCS run of a Q_u=48 normal grain growth model, following which the clock was reset to zero. The ratio of stored energy to grain boundary energy, H/J, was chosen to be either 3 or 5. Two types of nucleation were considered: site saturated and constant nucleation rate. For site saturated nucleation, a fixed number of nuclei were randomly placed in the microstructure and no additional new nuclei were created. Physically, this is equivalent to annealing the deformed metal at high temperature to create nuclei at time zero, then quenching to lower temperature such that growth takes place with no future nucleation. For the case of constant nucleation rate, a fixed number of nuclei were randomly placed in the microstructure after each Monte Carlo step. If a new nucleus was placed in a grain which had been recrystallized, that nucleus was removed. All nuclei which were added were of critical size. Spontaneous nucleation was not allowed to occur.

The microstructural evolution for recrystallization under conditions of site saturated and constant nucleation rate are shown in Fig. 2 and Fig. 3, respectively. A number of common features are observed. First, during the period of isolated growth the recrystallized grains grow at an identical rate and remain essentially circular. The boundaries are somewhat rough, and small regions of matrix are sometimes trapped behind the recrystallization fronts. However, as the boundaries continue to advance, the occluded regions are eventually recrystallized. Second, when impingement takes place irregular grain morphologies are sometimes created. This is exemplified by the elongated grains seen along the left edge of Fig. 2 (t=820). Third, after recrystallization is complete the microstructures still have excess energy with respect to normal grain growth conditions. Many of the grain boundaries do not intersect at 120 degrees (required for local equilibrium under conditions of isotropic grain boundary energy), and they are non-compact interfaces in the sense that they exhibit undulations.

There are also differences between the recrystallized microstructures for the two nucleation conditions. In the case of site saturated nucleation, the microstructure exhibits a relatively sharp grain size distribution. The final mean grain area is found to be inversely proportional to the initial nuclei concentration. In contrast, the grain size distribution obtained from a constant nucleation rate is broader due to continued nucleation of recrystallized grains as a function of time. The microstructure is topologically different in that it contains two sided grains, as shown on the right side of Fig. 3 (t=800). These grains occur when nucleation takes place between two larger pre-existing grains (a condition which is never met for site saturated nucleation). The final mean grain area is found to be inversely proportional to the nucleation rate to the 2/3 power. This is consistent with theoretical predictions by Gilbert (19) for a randomly nucleated microstructure.

The recrystallized volume fraction F was followed as a function of time, and is shown in Fig. 4 for site saturated nucleation in which H/J=3. Under all nucleation conditions, F is found to be a sigmoidal function of time, in agreement with experimental observation. The simulations show no incubation period for recrystallization. However, in the case that the experimentally detectable recrystallized grain size is finite, an apparent incubation period will exist.

The Avrami exponent p was evaluated for the different nucleation conditions from

$$p = \frac{\partial \log (\log (1/(1-F))}{\partial \log t} \qquad (5)$$

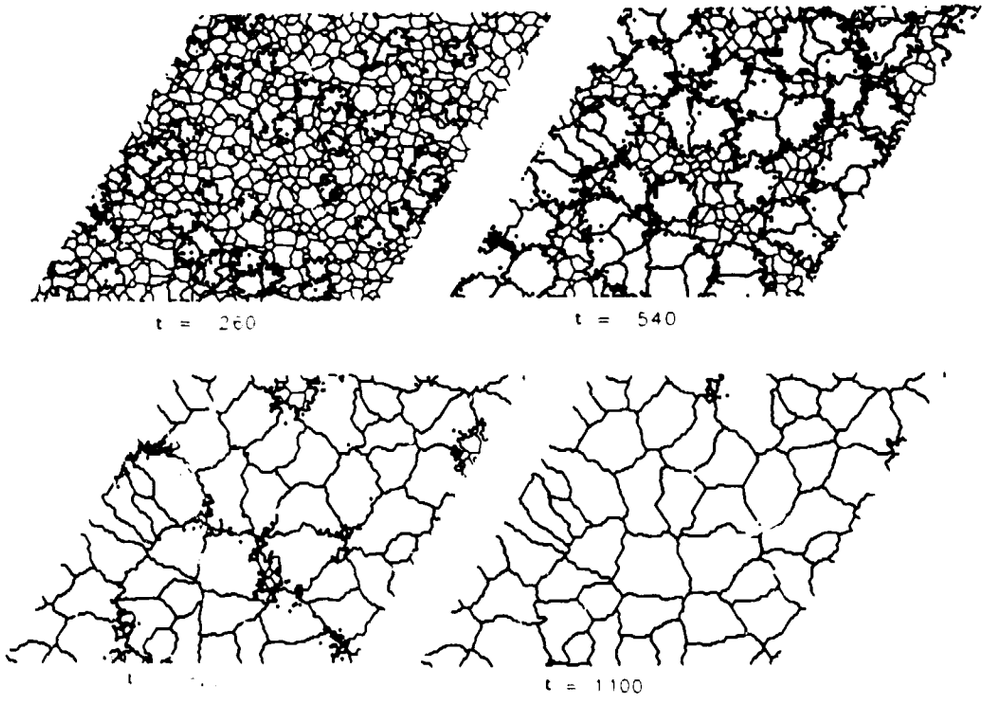

Fig. 2 The temporal evolution of the microstructure during homogeneous recrystallization under site saturated nucleation conditions (50 nuclei/40,000 sites) with H/J=3. The shaded grains have been recrystallized.

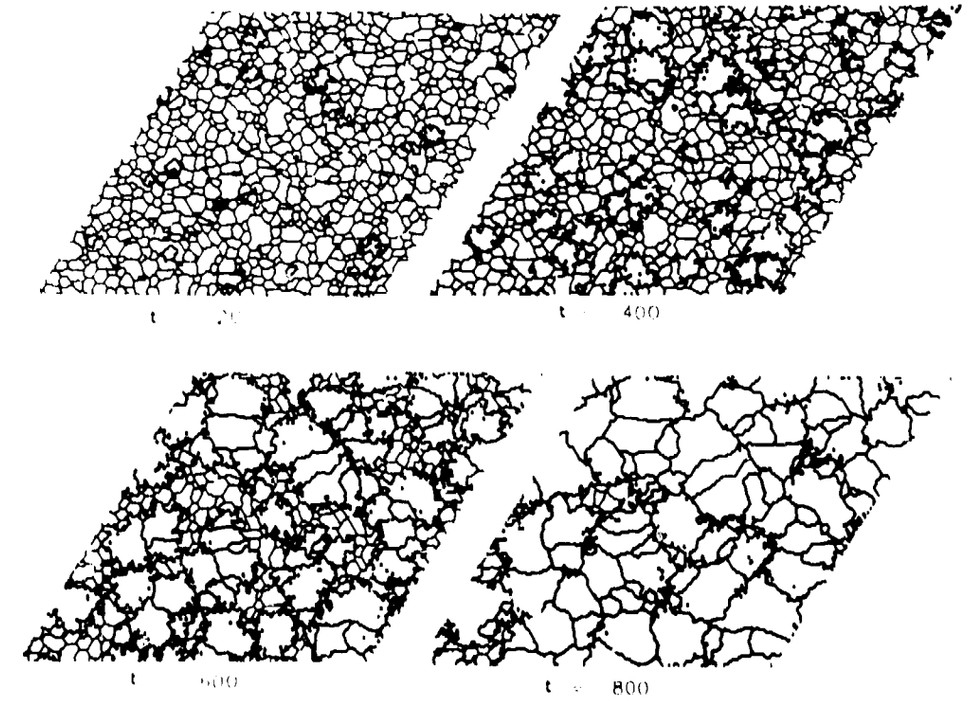

Fig. 3 The temporal evolution of the microstructure during homogeneous recrystallization under constant nucleation rate conditions (0.2 nuclei/MCS) with H/J=3. The shaded grains have been recrystallized.

Such a determination is shown in Fig. 5 for the data of Fig. 4. If the JMA equation is exactly obeyed, the data should fall on straight lines. It is found that, for both nucleation conditions, a small degree of curvature is

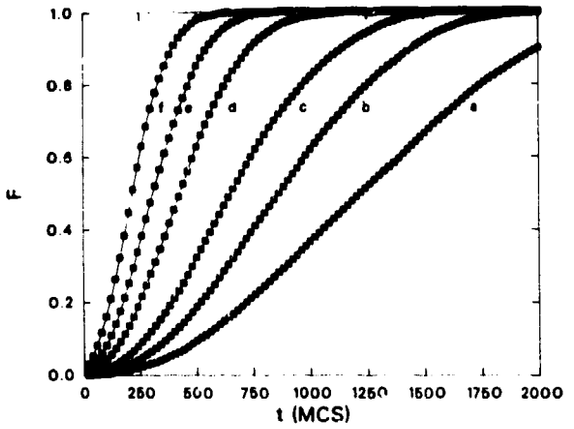

Fig. 4 The recrystallized area fraction, F, versus time during homogeneous recrystallization under site saturated nucleation conditions with H/J=3. Curves a-f correspond to 5, 10, 50, 100 and 200 nuclei/40,000 sites, respectively.

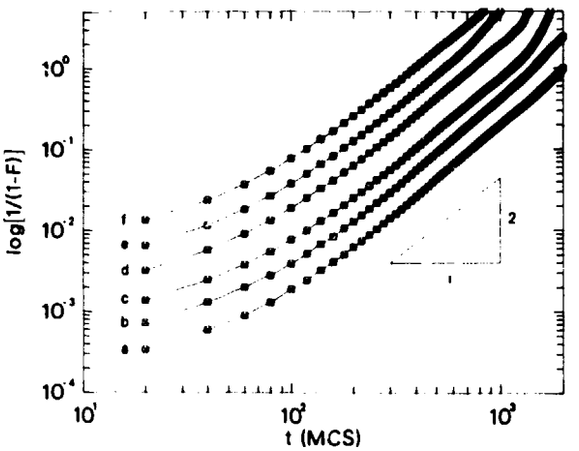

Fig. 5 Graphical representation of Eq. (5) for the data shown in Fig. 4. The triangle indicates the predicted slope for site saturated nucleation in two dimensions.

present, particularly at very short times. It is possible that the short time deviation is due to the departure from the linear relationship between recrystallized grain radius and time at small grain sizes. Theoretically, the growth rate for an individual recrystallized grain is given by

$$\frac{dR}{dt} = M\left(- C_1 \gamma/R + C_2\, \delta G\right) \qquad (6)$$

where M is the boundary mobility, γ is the grain boundary energy, δG is the stored energy R is the radius of the growing grain, and C_1 and C_2 are constants of order unity. For R sufficiently small, the growth rate is not constant but exhibits a size dependence. Best fits to the linear portions of the curves yield slopes of 2.3 ± 0.2 for site saturated nucleation, and 3.0 ± 0.2 for constant nucleation rate. These values are in fair agreement with the theoretically predicted exponents of 2 and 3, respectively.

The mean area of the recrystallized grains was also followed as a function of time. These data for site saturated nucleation in which H/J=3 are shown in Fig. 6. At short times for both nucleation conditions curvature is observed, demonstrating the non-linear R vs. t behavior at early times. However, with increasing time, linear behavior ensues, such that A varies with t^2 as expected. At later times the mean area saturates due to total grain

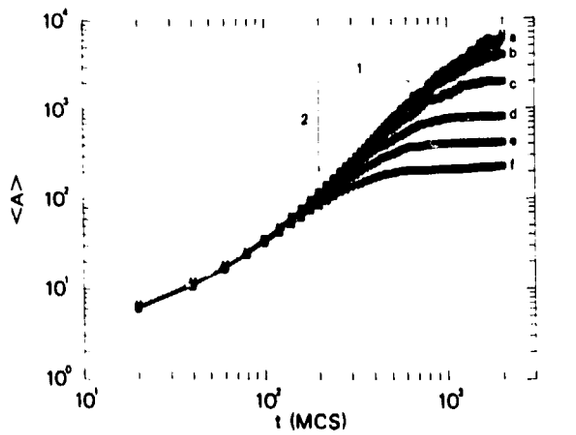

Fig. 6 The average recrystallized grain area, A, versus time for homogeneous recrystallization under conditions of site saturated nucleation with H/J=3. The slope of 2 indicated by the inset triangle represents the growth kinetics of a recrystallizing grain in a uniform background.

mpingement. The slope of A at saturation is much less than one, ndicating that normal grain growth has not yet begun. Presumably, local quilibration of vertices and boundary smoothing must take place before ormal grain growth can begin.

3. Heterogeneous Nucleation

The recrystallization of a polycrystalline matrix under conditions of eterogeneous nucleations was also investigated. By hetergeneous ucleation is meant that the degree of stored energy is too small to upport growth in a uniform background for an embryo of given size. uccessful nucleation (growth of the embryo) can only take place at re-existing heterogeneities in the microstructure. As before, the icrostructure was initialized by a 1000 MCS run of a Q_u=48 normal grain rowth model, following which the clock was reset to zero. The ratio of tored energy to grain boundary energy was chosen to be either 0.5, 1.0, .5, or 2.0. For these amounts of stored energy the critical embryo size equired for homogeneous nucleation is essentially infinite. Two types of ucleation were considered: site saturated and constant nucleation rate. s before, for site saturated nucleation a fixed number of nuclei were andomly placed in the microstructure, and no additional nuclei were reated. For the case of constant nucleation rate, a fixed number of uclei were randomly placed in the mirostructure after each Monte Carlo tep. If a new nucleus was placed in a grain which had been ecrystallized, that nucleus was removed. The size of the nucleus employed as three lattice sites.

The microstructural evolution for recrystallization under conditions f site saturated and constant nucleation rate are shown in Fig. 7 and 8, espectively. A number of differences with respect to homogeneous ucleation are observed. First, only embryos which are present on grain oundaries or grain boundary intersections grow. At the lowest stored nergy employed, successful nuclei are found exclusively on grain ertices. As the stored energy is increased, successful nucleation then egins to occur on the two-grain interfaces (grain boundaries). Embryos hich are present in the grain interiors shrink and disappear. During rowth, the boundaries of th recrystallized grains are smoother than for omogeneous nucleation, and occlusion of unrecrystallized matrix does not ccur. Second, the growth rates of the recrystallized grains before mpingement are not identical; some grains grow faster than others. This s most obvious in the case of site saturated nucleation (Fig. 7), where 11 nuclei start at time zero with the same initial size. Third, while mpingement still leads to some irregular grain morphologies, the ecrystallized grain shapes tend to be much more equiaxed than for omogeneous nucleation. Fourth, after recrystallization is complete the rain boundary configuation is much closer to the normal grain growth state han for homogeneous nucleation. The boundaries are much more compact in hat they do not have the undulations found above, and many intersect at 20 degrees (satisfying local equilibrium).

There are also similarities with respect to homogeneous nucleation. he grain size distribution is sharper for site saturated nucleation in omparison to constant nucleation rate, as previously observed. The opological differences between site saturated and constant nucleation rate re still present (e.g. the occurrence two-sided grains).

The recrystallized volume fraction F was followed as a function of ime, and is shown in Fig. 9 for constant nucleation rate in which /J=0.5. Under both nucleation conditions, F is again found to be a igmoidal function of time, except for site saturated nucleation at the

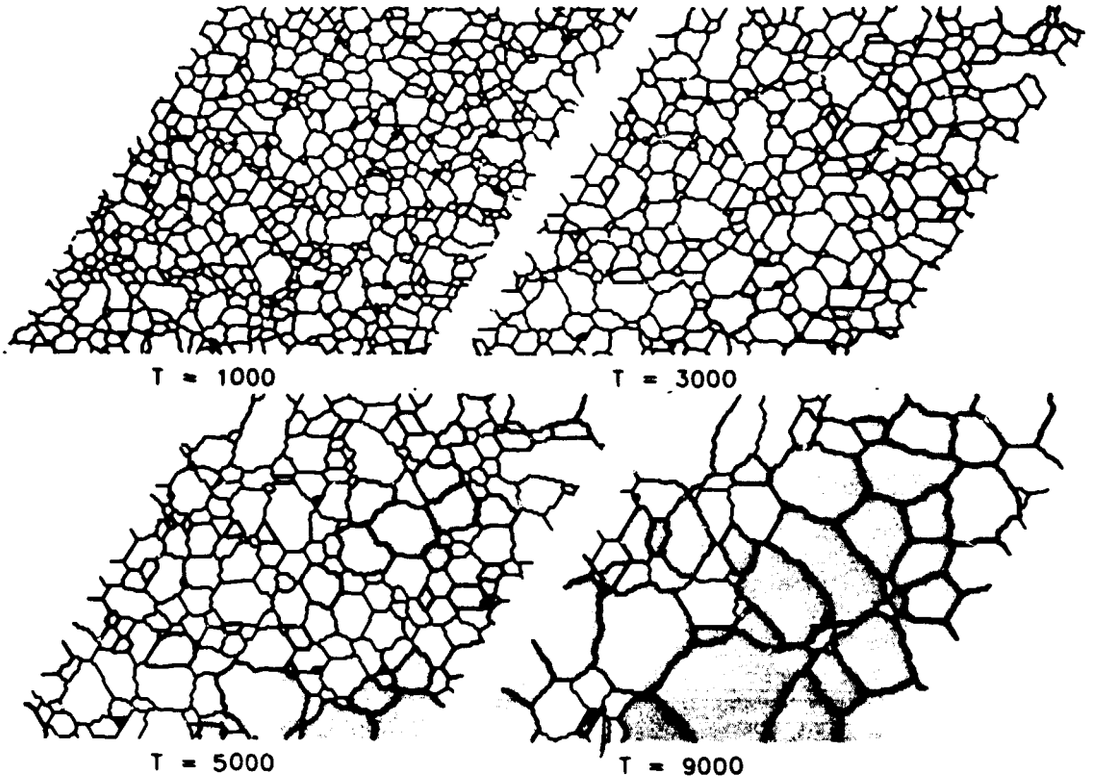

Fig. 7 The temporal evolution of microstructure during heterogeneous recrystallization under site saturated nucleation conditions (500 nuclei/40,000 sites) with H/J=0.5.

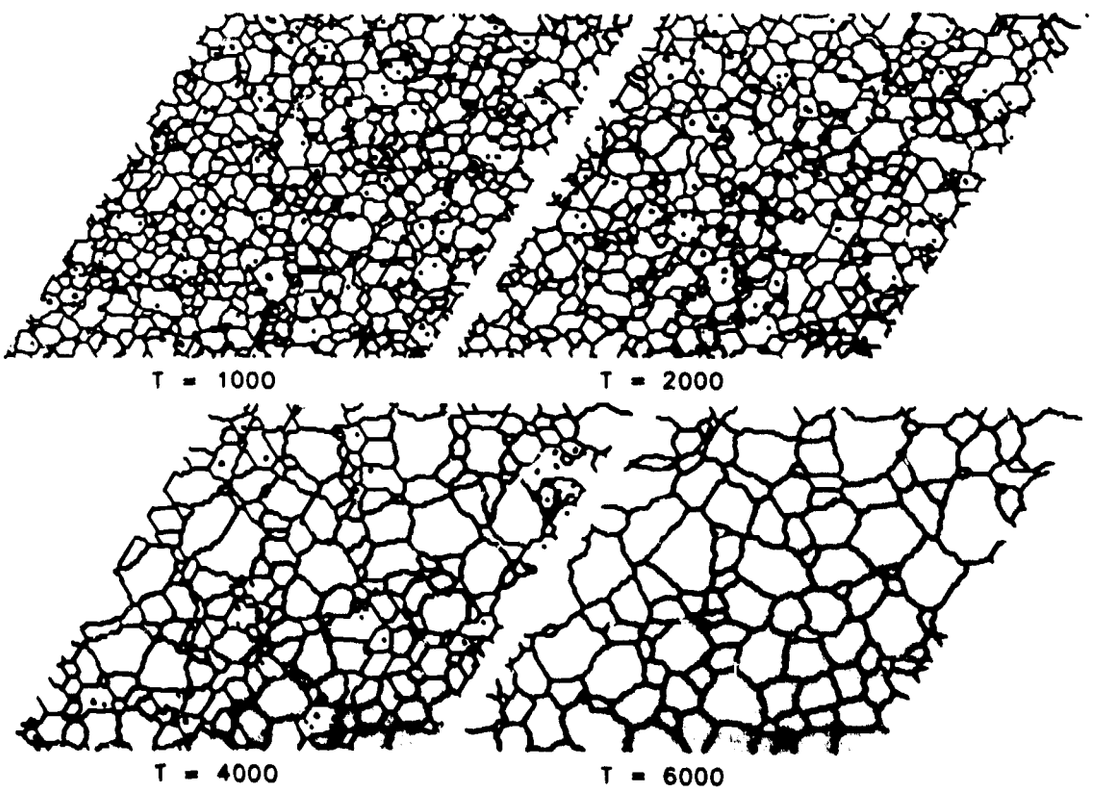

Fig. 8 The temporal evolution of microstructure during heterogeneous recrystallization under constant nucleation rate conditions (3 nuclei/MCS) with H/J=0.5.

lowest value of stored energy. In this case a small dip is observed at short times due to the elimination of unsuccessful embryos. At long times the sigmoidal behavior is recovered. As before, the simulations show no incubation period for recrystallization.

The recrystallized volume fraction was plotted in accordance with Eq. 5 to check the validity of the JMA analysis. These results are shown in Fig. 10 for the data of Fig. 9. Unlike for homogeneous nucleation,

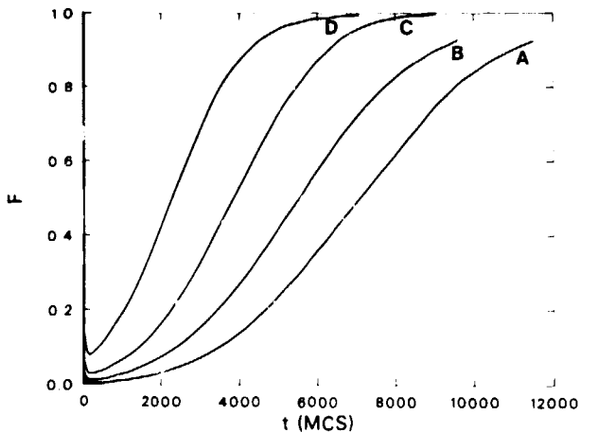

Fig. 9 The recrystallized area fraction, F, versus time during heterogeneous recrystallization under conditions of site saturated nucleation for H/J=0.5. Curves a-d correspond to 200, 500, 1000, and 2000 nuclei/40,000 sites, respectively.

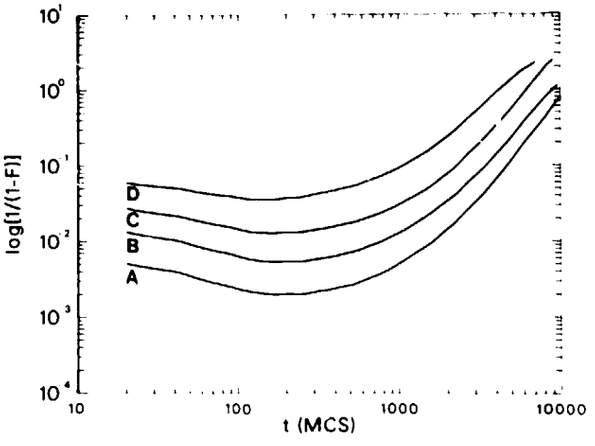

Fig. 10 Graphical representation of Eq. (5) for the data of Fig. 9.

significant deviations from linearity are observed. No attempt was made to fit the data for an Avrami exponent. The substantial violation of linearity may be a consequence of the different growth rates exhibited by the recrystallized grains. In the JMA analysis, it is assumed that all grains grow at identical rates. The variable growth rate observed is thought to be a consequence of two factors. First, a non-linear dependence of growth rate on size beyond that predicted by Eq. 6. Second, a dependence of growth rate on details of the local environment at small size. Growth appears to occur by motion of the vertices of the recrystallized grain along pre-existing boundaries. Consequently, at small size the growth rate will be substantially affected by the number of vertices the embryo has.

B. Secondary Recrystallization

The occurrence of secondary recrystallization in a microstructure where primary recrystallization is complete has been attributed to a number of sources. These sources can be divided into two types by dominant driving force. The first possible source is traced to instabilities which are predicted to occur in grain growth where the driving force is provided solely by curvature (10-12). The growth instabilities are triggered in one of three ways:

(a) If an abnormally large grain (greater than 2R in 2d or 9/4 R in 3d) is introduced into the grain ensemble in a system free from grain growth restraints.
(b) If particle retardation of grain growth takes place but the Zener drag is small and the system has not completely pinned.

(c) If the microstructure is completely pinned by particles but a time dependent decrease in Zener drag (through a reduction in the number of particles by dissolution or Ostwald ripening) takes place.

The models used to make these predictions assume that grains are spherical and growing in an average environment.

The second possible origin for secondary recrystallization is the presence of volume (3d) or area (2d) distributed energies, which provide driving forces in addition to that due to curvature (13-15). Local differences in these energies then lead to abnormal grain growth, characterized by boundary migration behavior similar to that found in primary recrystallization. The sources of the additional driving forces include elastic strain, residual dislocation density, and (in 2d) differences in surface energy.

In this part of the paper we review simulations (17) in which both these hypotheses are tested.

1. Curvature Driven Growth

The first simulations performed investigated the stability of the grain size distribution function developed during normal grain growth. In this case H=0 in Eq. (4). A microstructure produced by a 1000 MCS run of a Q=48 normal grain growth model was modified by artificially creating a large circular grain in its center. Initial circular grain sizes of 5, 10, 15, and 20 times the mean grain radius was used. The resulting microstructural development is shown in Fig. 11 for the case where $R_0/\bar{R}$ is

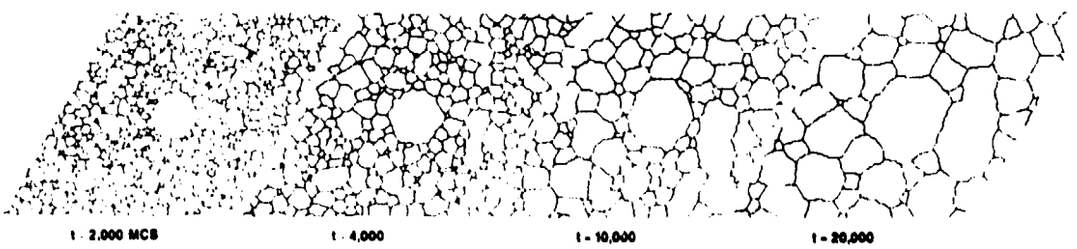

Fig. 11 The growth of a large grain in an otherwise normal grain growth microstructure.

initially 5. R_0 is the radius of the large circular grain, and $\bar{R}$ is the average grain radius excluding the large grain. The ratio of the area of the large grain, A_0, to the mean grain area excluding the large grain, $\bar{A}$, as a function of time is given in Fig. 12. These data show that the abnormal grain is a temporary feature of the microstructure. That is, the abnormal grain grows at a rate slower than the remainder of the microstructure until it is absorbed into the normal grain size distribution.

Since abnormally large grains do not of themselves lead to abnormal grain growth, simulations were performed in the presence of particle dispersions. In these simulations grain growth was allowed to occur in microstructures containing particles until stagnation took place. Following complete pinning, two different experiments were performed.

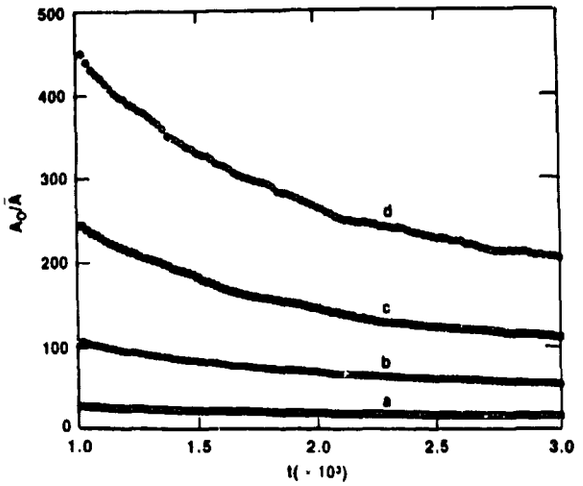

Fig. 12 The time dependence of the ratio of the areas of the large grain, A_0, to the mean grain area, $\bar{A}$. The data is presented for initial large grain radii (at 1,000 MCS) of (a) 5, (b) 10, (c) 15, and (d) 20 $\bar{R}$.

First, the concentration (area fraction) of particles was uniformly reduced from 2.5% to 1.5%, and the simulation was re-started. Second, all the particles were removed from one part of the microstructure to create a particle-free region, and the simulation was re-started. The time evolution of this microstructure is shown in Fig. 13.

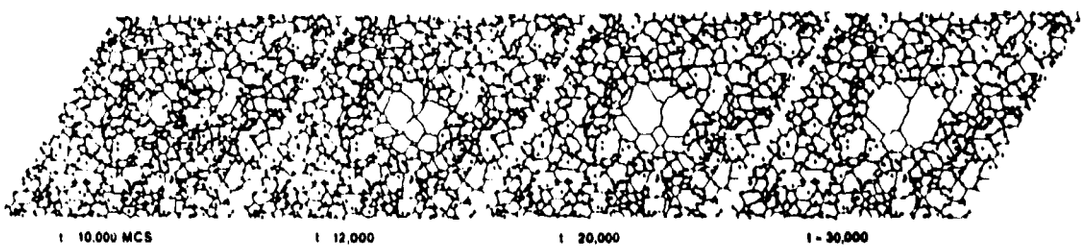

Fig. 13 Temporal evolution of a pinned microstructure following the removal of a large group of particles from one area.

For all these cases, while short growth transients were observed, pinning eventually took place and abnormal grain growth was not initiated.

2. Surface Energy Driven Growth

To test the second hypothesis concerning the origin of secondary recrystallization, simulations were carried out with H=0.10 in Eq. (4). In these studies, a normal grain growth microstructure produced by a 1000 MCS run of a Q=48 model was re-labeled so that each grain had a unique orientation. A fraction f of the grains was then selected as initial secondaries. f was chosen as either 2%, 5%, 10%, or 20%.

Figure 14 shows the microstructural evolution of a structure where initially 2% of the grains were secondaries. It is seen that the secondaries grow at a much more rapid rate than do the matrix grains, and that after a relatively short period of time the entire microstructure is composed of secondary grains. This behavior is similar to that of primary recrystallization discussed above. In contrast to the homogeneous nucleation recrystallization model, however, the secondary grain boundaries remain smooth and no occluded regions are formed. After secondary recrystallization is complete, the microstructure is much closer to the normal grain growth state in that the grain shapes are compact and the boundary intersections are close to 120 degrees.

Figure 16 presents the temporal evolution of the grain size distribution function during secondary recrystallization. At t=0, the grain size distribution function is just the normal grain growth distribution function. At intermediate times, the grain size distribution function consists of the large secondary grains and the much smaller matrix grains. This results in a broad grain size distribution, as experimentally observed. When the transformation is complete, the secondary grains compete against each other by normal grain growth and the size distribution assumes the same width as before the onset of abnormal grain growth.

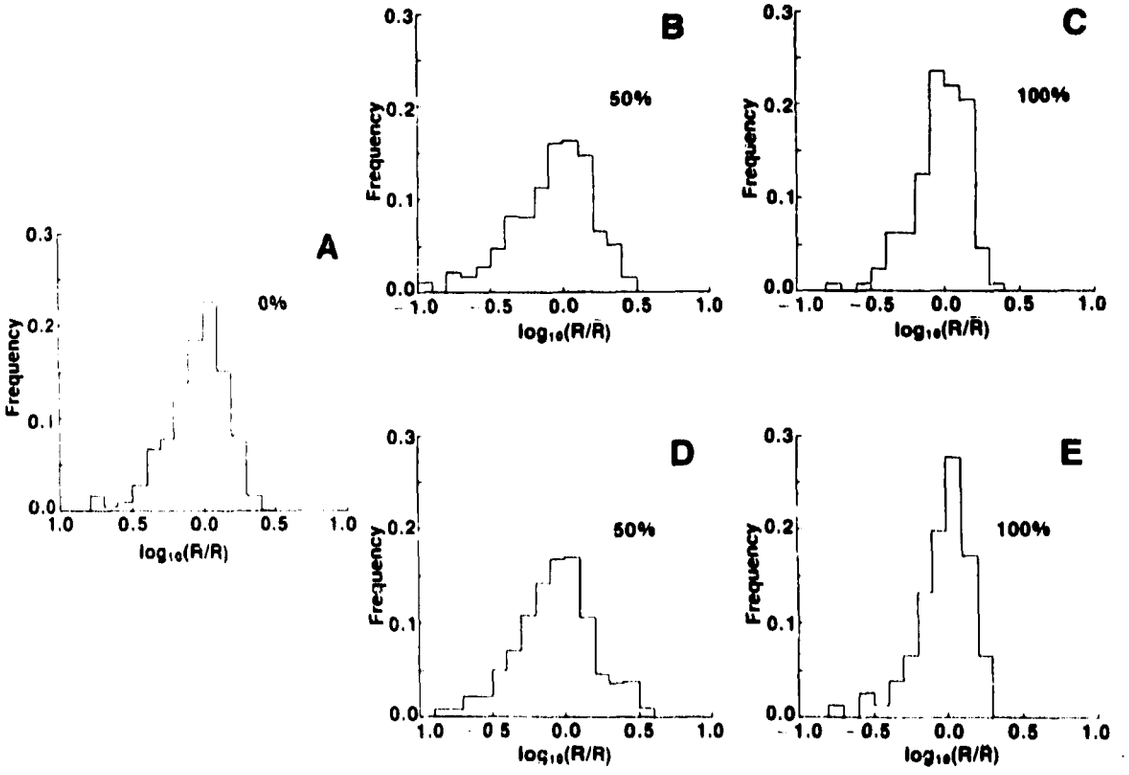

Fig. 16 The grain size distribution corresponding to (a) a normal grain growth microstructure at 1,000 MCS. Figures b and c correspond to the microstructure having initially (t=1,000 MCS) 2% secondary grains for X = 50% and 100%. Figures d and e are corresponding distributions for the microstructure having initially 10% secondary grains for X = 50% and 100%.

Summary

A simple and general simulation technique has been developed which easily lends itself to the analysis of complex microstructure. The technique has been applied to the problem of primary and secondary recrystallization.

Primary recrystallization has been modelled under conditions where the degree of stored energy is varied and nucleation occurs either homogeneously or heterogeneously. The nucleation rate is chosen as either constant or site saturated. As the degree of stored energy is increased, a number of changes take place in the characteristics of the recrystallized grains. First, the locations where successful nucleation occur increase in number to progressively include grain boundary vertices, two-grain interfaces (grain boundaries), and ultimately grain interiors. Second, the

boundaries of the growing grains change from being relatively smooth to rough, with a greater tendency to trap unrecrystallized matrix behind the recrystallization front. Third, the growth rate for different recrystallized grains changes from being non-uniform to essentially identical. Fourth, the morphology of grains in the recrystallized microstructure changes from equiaxed to a greater irregularity of shape (elongated). The final grain boundary configuration departs increasingly from that of a normal grain growth state in that interfaces become non-compact (undulate) and boundary intersections increasingly deviate from 120 degrees.

For all of the recrystallization conditions studied, the recrystallized volume fraction exhibits sigmoidal variation with time. Only the homogeneous nucleation data, however, are approximately fit by the Johnson-Mehl-Avrami equation with the expected exponents. Significant departures from the JMA relationship are found in the case of heterogeneous nucleation. This is attributed to the non-uniform growth rate exhibited by the recrystallized grains at low stored energy and small size. Under conditions of site saturated nucleation, the recrystallized microstructure is characterized by a relatively sharp grain size distribution. In contrast, for constant nucleation rate, the grain size distribution is broader and the density of two-sided grains increases.

Secondary recrystallization has been modelled under two conditions: (a) where the driving force is provided solely by curvature and (b) where the driving force is provided by the difference in the solid-vapor surface energy between grains of different crystallographic orientation. For curvature driven growth three cases are considered: (a) the growth of abnormally large grains in recrystallized microstructures without grain growth restraints, (b) the growth of abnormally large grains in microstructures with particle dispersions, and (c) grain growth in a particle pinned microstructure in which a decrease in the number of particles occurs. In all these cases, the initiation of secondary recrystallization is not found to occur. In systems free from grain growth restraints the normal grain size distribution is very robust and strongly resistant to perturbations. For systems which contain particle dispersions strong pinning of the grain boundaries is always observed. However, when a preferred surface energy orientation is introduced, secondary recrystallization does take place. The microstructural evolution observed during secondary recrystallization is in good correspondence with experiment. The volume fraction of secondary grains exhibits sigmoidal behavior as a function of time, and is fit by the JMA equation.

References

1. M. P. Anderson, D. J. Srolovitz, G. S. Grest and P. S. Sahni, Acta Metall. 32, 783 (1984).
2. D. J. Srolovitz, M. P. Anderson, P. S. Sahni and G. S. Grest, Acta Metall. 32, 793 (1984)
3. G. S. Grest, M. P. Anderson and D. J. Srolovitz, "Computer Simulation of Microstructural Dynamics", this volume.
4. F. Haessner, "Recrystallization of Metallic Materials" (edited by F. Haessner), Dr. Riederer Verlag GmbH, Stuttgart (1978), p. 2.
5. J. G. Byrne, "Recovery, Recrystallization, and Grain Growth", MacMillan, New York, NY (1965), p. 60.
6. W. A. Johnson and R. F. Mehl, Trans. AIME 135, 416 (1939).
7. M. Avrami, J. Chem. Phys. 7, 1103 (1939); ibid. 8, 212 (1940); ibid 9, 177 (1941).
8. F. Haessner, "Recrystallization of Metallic Materials" (edited by F. Haessner), Dr. Riederer Verlag GmbH, Stuttgart (1978), p. 3.

9. K. Detert, "Recrystallization of Metallic Materials" (edited by F. Haessner), Riederer Verlag, Stuttgart (1978), p. 97.
10. M. Hillert, Acta Metall. 13, 227 (1965).
11. O. Hunderi and N. Ryum, Acta Metall. 29, 1737 (1981).
12. O. Hunderi and N. Ryum, Acta Metall. 30, 739 (1982).
13. J. L. Walter and C. G. Dunn, Acta Metall. 8, 497 (1960).
14. F. H. Buttner, E. R. Funk and H. Udin, J. Phys. Chem. 56, 657 (1952).
15. D. Kohler, J. Appl. Phys. 31, Suppl., 408S (1960).
16. D. J. Srolovitz, G. S. Grest and M. P. Anderson, Acta Metall., submitted.
17. D. J. Srolovitz, G. S. Grest and M. P. Anderson, Acta Metall. 33, 2233 (1985)
18. H. P. Stuwe, "Recrystallization of Metallic Materials" (edited by F. Haessner), Dr. Riederer Verlag GmbH, Stuttgart (1978), p.12.
19. E. N. Gilbert, Ann. Math. Stat. 33, 958 (1962).